LIMNOLOGY
and
OCEANOGRAPHY: METHODS

ASLO

Limnol. Oceanogr.: Methods 17, 2019, 277–291

doi: 10.1002/lom3.10312

Improved ultraviolet photo-oxidation system yields estimates for deep-sea dissolved organic nitrogen and phosphorus

Rhea K. Foreman,[1]* **Karin M. Björkman**,[1] **Craig A. Carlson**,[2] **Keri Opalk**,[2] **David M. Karl**[1]

[1]Daniel K. Inouye Center for Microbial Oceanography: Research and Education, Department of Oceanography, School of Ocean and Earth Science and Technology, University of Hawaii at Manoa, Honolulu, Hawaii

[2]Department of Ecology, Evolution and Marine Biology and Marine Science Institute, University of California, Santa Barbara, California

Abstract

Photolysis of dissolved organic matter using high-intensity, ultraviolet (UV) light has been utilized since the 1960s as a method for the oxidation and subsequent quantification of dissolved organic nitrogen and phosphorus (DON and DOP) in both freshwater and marine water. However, conventional UV systems yielded variable and sometimes unreliable results; consequently, the method fell out of favor throughout much of the oceanographic community. Researchers turned to other oxidation methods such as persulfate oxidation or high-temperature combustion, even though they have difficulty when DON and DOP are <10% of the total dissolved N and P (for example, in the deep sea and in surface waters at high latitudes). Here, we revive the UV oxidation method using modernized light-generating equipment and high-precision colorimetric analysis of the oxidation products, resulting in the most well-constrained full ocean depth profiles of DON and DOP that are available to date. At Station ALOHA, in the North Pacific Subtropical Gyre, in the depth range of 900–4800 m, we find that DON is 2.2 ± 0.2 μmol L^{-1} ($n = 49$), DOP is 0.049 ± 0.004 μmol L^{-1} ($n = 19$), and the DOC : DON : DOP molar stochiometric relationship is 759 : 45 : 1. Preliminary estimates for the global ocean inventories of refractory DON and DOP are placed at 43.6 Pg N and 2.14 Pg P.

The biogeochemical cycling of dissolved organic matter (DOM)—its formation, consumption, alteration, and degradation—most fundamentally represents the transformations of energy and matter in marine ecosystems. Microorganisms are the primary mediators of DOM fluxes in the oceans and so, from many perspectives, discussions of DOM are implicit discussions of microbial oceanography. In a recent paper entitled "The global ocean microbiome," Moran (2015) coined the various molecules of DOM the "currencies" of microbial activity.

The inventory of carbon stored as DOM in the global ocean (662 Pg C; Hansell et al. 2009) is on par with the carbon inventory of the atmosphere, and, accordingly, marine DOM is gaining recognition as a crucial part of the Earth's carbon cycle. Many questions about DOM remain unanswered, such as which organisms produce, transform, or consume which compounds? What are the associated residence times and reactivities of different DOM fractions? Which compounds are most informative of microbial community structure, health, and functioning? At the most fundamental level, what are the budget, distribution, and elemental composition of DOM in the oceans? In addition to ecological inquiries, it is becoming clear that a deeper understanding of DOM is needed in order to detail and predict how modern global change might perturb this reservoir (e.g., Ridgewell and Arndt 2015).

To address these expansive questions, many studies of DOM focus on three of the most essential building blocks of life, carbon (C), nitrogen (N), and phosphorus (P), with the goals being to (1) quantify their total concentrations and how their stoichiometric relationship changes in space and time and (2) identify individual or classes of organic compounds that comprise DOM. Resolving the dynamics of individual compounds is of obvious value, and mysteries of the sea have indeed been solved with this approach, such as the recent discovery of aerobic methanogenesis via bacterial degradation of methylphosphonates (Karl et al. 2008; Repeta et al. 2016). However, the scope of the present work is concerned with goal number one. Some questions, such as those concerning fluxes or residence times, cannot be answered without a precise understanding of total elemental budgets, distributions, and speciation in the four dimensions of space and time.

Dissolved organic carbon, nitrogen, and phosphorus (DOC, DON, and DOP, respectively), each a puzzle piece of whole DOM, are quantified through oxidation of the organic molecules

*Correspondence: rforeman@hawaii.edu

Additional Supporting Information may be found in the online version of this article.

and analysis of the mineralization products, effectively turning myriad, unresolvable compounds into quantifiable units for each of the elements in question. The oxidation step can be achieved through high-temperature combustion (HTC), wet chemical oxidation, or photo-oxidation using ultraviolet (UV) light (*see* reviews by Karl and Björkman [2015] and Sipler and Bronk [2015]). For DON and DOP, the oxidation step converts all organic and inorganic molecules to the same oxidized species, so the parameters that are quantified analytically after oxidation are the total dissolved nitrogen and phosphorus (TDN and TDP). Hence, DON and DOP are never measured directly, but instead are calculated as the difference between TDN or TDP and their inorganic counterparts, which are typically dominated by nitrate and nitrite (NO_3^- and NO_2^-, herein referred to as N + N) and orthophosphate (PO_4^{3-}), respectively, in most marine environments.

Over the last few decades, there have been great advances in knowledge in quantifying the global distribution of DOC using the HTC method (Hansell and Carlson 1998). This important advance is made possible by: (1) innovations in instrumentation, (2) standardization of procedure and the use of reference materials, (3) the fact that DOC occurs in high concentrations (35–80 μmol L^{-1} throughout the oceans; Hansell et al. 2009) and (4) because DOC can be analytically decoupled from dissolved inorganic carbon (DIC) through acidification of a water sample and the purging of all DIC as carbon dioxide prior to the oxidation of organic carbon. These factors combined have resulted in a high-precision DOC dataset for the world's oceans. The same cannot be said for DON or DOP; concentrations are much lower (typically <6 μmol L^{-1} for DON [Sipler and Bronk 2015] and <0.5 μmol L^{-1} for DOP [Karl and Björkman 2015]) and no analytical method currently exists for selectively removing inorganic N or P—before oxidation—without disturbing the pool of organics.

In a typical open ocean profile in tropical to temperate latitudes, DOC, DON, and DOP concentrations are greatest at the surface. With increasing time (and depth), DOM is mined of its nutritional value by microbial activity, resulting in decreasing C, N, and P concentrations and the formation of compounds that are more refractory, C-rich, and harder to degrade further (Loh and Bauer 2000; Karl et al. 2001; Aminot and Kérouel 2004; Letscher and Moore 2015). Most DON and DOP estimates are from the epipelagic zone (Torres-Valdés et al. 2009; Letscher et al. 2013; Sipler and Bronk 2015; Karl and Björkman 2015) where inorganic nutrients are at their lowest concentrations and organic nutrients are at their highest concentrations, translating to the lowest error in the difference calculation. There are very few reliable DON or DOP estimates in waters deeper than 1000 m due to large analytical uncertainties. Therefore, it is safe to say that the distribution of organic N and P is not well-known for ~80% of the open ocean.

Early work on the photolytic determination of organic compounds in water was conducted by Beattie et al. (1961), followed shortly by Armstrong et al. (1966) and Armstrong and Tibbitts (1968) for DOC, DON, and DOP in seawater. Together, these contributions provided the groundwork for the next 50+ years of data collection using UV oxidation. Although some studies have shown great success with the UV method, there are several issues that we believe have contributed to skepticism concerning photo-oxidation, including: (1) results are highly dependent on procedural details (e.g., Ridal and Moore 1990) that can vary from lab to lab without sufficient validation; (2) yields are highly variable both between studies and within a single study (Sharp et al. 2002); (3) it is well-known that certain compounds are difficult to photo-oxidize, such as urea (Armstrong et al. 1966; Walsh 1989) and polyphosphates (Thomson-Bulldis and Karl 1998); and (4) UV equipment can perform unreliably due to aging bulbs or inefficient/heterogeneous light distribution (Bronk et al. 2000).

To increase the precision and reliability of DON and DOP estimates, we use a modernized, UV photo-oxidation system coupled with back-to-back colorimetric analyses of TDN with N + N and TDP with soluble reactive phosphorus (SRP, which is predominantly PO_4^{3-}). The result is highly consistent recovery and reproducibility of TDN and TDP, leading to well-constrained estimates for deep-ocean DON and DOP concentrations near Station ALOHA in the North Pacific Subtropical Gyre, and home to the Hawaii Ocean Time-series (HOT) program (Karl and Lukas 1996; http://hahana.soest.hawaii.edu/).

Materials and procedures

UV irradiance assembly

We use a VelaCure12 UV light system (*see* Supporting Information for photos) that was originally designed for three-dimensional curing or sterilization (available with customizable options from DDU Enterprises, http://www.doctoruv.com, or VelaUV, http://www.velauv.com). Light is generated from a 6 in., 1800 W, microwave-powered, mercury lamp from Heraeus Noblelight (F300S lamp system with an H^+ bulb, Dichroic Plus reflector and P300MT power supply). The lamp unit directs light into a sample chamber of 12 in. × 12 in. × 12 in. internal dimensions that has a highly UV-reflective, proprietary coating. This results in very efficient and extremely uniform light capture by the sample vials, unlike a conventional photo-oxidation system in which UV irradiance is unidirectional from a central bulb and much of the UV energy is lost to the surroundings. The F300S lamp unit is isolated from the sample chamber by a frosted Suprasil quartz window, allowing cooling air to be directed across the lamp but not the samples. In addition to an integrated blower, the lamp is cooled by an exhaust fan placed inside a fume hood, which safely vents ozone generated by the bulb and is connected to the lamp unit with ~2 m of heat resistant, 3 in. diameter ducting. For TDP analyses, an additional step is taken to cool the samples themselves (*see* discussion below about silica dissolution and subsequent interference on phosphate analyses) by flowing

compressed air through an ice bath and into the 1/4 in. back port of the sample chamber at 20 psi; the second 1/4 in. back port is used as a vent by attaching a coil of 1/4 in. Fluorinated ethylene propylene (PET) tubing wrapped in black electrical tape to prevent UV light leaks. The two back ports are plugged for TDN runs.

Irradiance inside the sample chamber is monitored using an EIT Power Puck II radiometer at four different bandwidths: visible light (395–445 nm); UV-A (320–390 nm); UV-B (280–320 nm); and UV-C (250–260 nm). The radiometer is placed in the built-in side door of the light chamber, and irradiance readings, using 15 s of light exposure, are taken at the beginning of every oxidation run to ensure proper operation of the equipment. Typical irradiance values for a chamber filled with 24 samples, as in TDN, and 18 samples, as in TDP, are shown in Table 1. The difference between a full and empty chamber indicates how much light is being absorbed by the samples. One important advantage of microwave-powered, electrodeless bulbs is their consistent light output over a very long lifetime (at least 8000 h of operation, according to Heraeus Noblelight); in accordance, we have found extremely consistent performance of our UV system (even with different bulbs) as long as the chamber walls are kept dust-free by regular cleaning with deionized water. In addition to daily radiometer readings, performance of the UV light system is evaluated by including reference seawater samples as check standards with every sample set.

Sample handling

Custom sample vials for UV photo-oxidation were fabricated by Allen Scientific Glass from Suprasil 310 or GE 214 premium quartz glass tubing, chosen for their outstanding transmission of the entire UV-C spectrum, which provides the most energetic wavelengths of light, but is also the most difficult to transmit. The vials were assembled from a 12 cm length of 20 mm O.D. × 17 mm I.D. tubing mated to a 5 cm commercial quartz glass disk at the base and quartz glass screw threads (GL-18) at the top. Vials are closed using a Duran screw cap with a PTFE protected seal.

For the TDP and TDN analyses, vials were soaked in 10% HCl, rinsed 3–4 times with high-purity, 18.2 MΩ-cm, deionized water, and air dried. For TDN analyses only, vials were additionally cleaned by combusting at 450°C for 5 h. After cleaning, 20 mL of sample was poured directly into the quartz vials, to which 50 μL of 30% hydrogen peroxide (ACS grade, Fisher #H325-500) was added before capping for both TDN and TDP analyses. For TDP analyses, 9 μL of 5 N sulfuric acid (made with ACS Plus grade, Fisher #A300-212) was also added to each vial in order to prevent the dissolution of quartz glass, which interferes with the detection of phosphate (*see* Analytical Methods section). Caps were covered with PTFE tape to prevent overheating of samples (by increasing reflectance) as well as to protect the caps from degrading. Oxidation times were 8 h for a batch of 24 TDN samples and 1.5 h for a batch of 18 TDP samples. Temperatures of the sample vials, measured with an infrared thermometer gun (VWR #12777–846), equilibrate to 80°C ± 5°C for TDN and 50°C ± 2°C for TDP during the irradiation period.

Table 1. Typical irradiances inside the UV chamber measured with an EIT Power Puck II radiometer.

	UV-A (mW cm^{-2})	UV-B (mW cm^{-2})	UV-C (mW cm^{-2})	Vis (mW cm^{-2})
Empty	277	220	44	241
TDP	164	99	10	148
TDN	172	85	9.5	161

Once samples were irradiated, the concentrations of the mineralization products N + N and SRP were confirmed to be stable for at least 2 wk (the maximum time we tested) if the vials remain unopened and stored at room temperature, presumably because of sterility.

Analytical methods

Colorimetric analyses for N + N and TDN are made following Strickland and Parsons (1972) and adapted for segmented flow on a SEAL Analytical (formerly branded Bran Luebbe) AutoAnalyzer III with a high-resolution detector. Nitrate is quantitatively reduced to nitrite in a copperized cadmium reduction column buffered with ammonium chloride at pH 8.5. Nitrite is subsequently reacted with a mixed-color reagent consisting of phosphoric acid, sulfanilamide, and *N*-(1-naphthyl)ethylenediamine dihydrochloride. Light absorbance due to the formation of an azo dye is then detected at a wavelength of 550 nm. This method has a limit of quantification of ~75 nmol L^{-1} N + N and an average repeatability of 0.4%. Accuracy is determined by daily measurements of the Wako CSK standard nitrate solutions at 40.0 μmol L^{-1} N (Wako #037-10241) and 5.0 μmol L^{-1} N (Wako #036-10191); over the course of this study, we obtained average values of 39.88 ± 0.26 (1σ) and 4.99 ± 0.10 (1σ) μmol L^{-1} N for the two reference standards, respectively. For a given sample, TDN and N + N are analyzed back-to-back in duplicate to obtain the highest possible precision of their difference, and DON is calculated as (TDN − [N + N]). Ammonium concentrations should also be subtracted from TDN for a true calculation of DON, but they are ignored here because ammonium concentrations in the vicinity of Station ALOHA are generally below 20 nmol L^{-1} for the entire water column (Curless et al. 2017) and not statistically significant to the DON calculation. High sensitivity N + N analyses (<0.5 μmol L^{-1}) in seawater from the upper ~100 m of water depth was determined using the chemiluminescent method described in detail in Foreman et al. (2016) with a detection limit of 1 nmol L^{-1}.

As a comparison, TDN was also determined independently via the HTC method (Walsh 1989) on a modified Shimadzu TOC-V with attached Shimadzu TNM-1 at the University of California, Santa Barbara. Carrier gas was produced with a

Balston gas generator at 168 mL min^{-1} flow rate, and ozone (O_3) was generated by the TNM-1 unit at 0.5 L min^{-1} flow rate. Three to five replicates of 100 μL of sample were injected into the combustion tube heated to 720°C, where the TN in the sample was converted to nitric oxide (NO). The resulting gas stream then passed through an electronic dehumidifier, halide trap, 0.2 μm filter, and a chemiluminescence analyzer, where the dried NO gas reacted with O_3 to produce an excited nitrous oxide. The resulting chemiluminescent signal was detected with a Shimadzu TNM-1 detector, and peak area was integrated with Shimadzu chromatographic software. For every HTC TDN sample analysis, calibration was achieved using potassium nitrate solutions (3–48 μmol L^{-1} N) in nanopure deionized water, and accuracy was confirmed using internal reference waters and/or consensus reference material (natural seawater with 4–45 μmol L^{-1} N) provided by D. Hansell's Organic Biogeochemistry Laboratory at the University of Miami (Hansell 2005). Analytical precision is typically ~0.5 μmol L^{-1} TDN or a coefficient of variation (CV) of ~5% to 10%. Additional details can be found in Letscher et al. (2013).

Colorimetric analyses for SRP and TDP were made on a SEAL Analytical AutoAnalyzer III with a high-resolution detector using the chemistry of Murphy and Riley (1962). In a sulfuric acid medium with sodium dodecyl sulfate surfactant, a blue phosphomolybdenum complex is generated with a mixed color reagent consisting of antimony potassium tartrate, ammonium molybdate, and ascorbic acid; light absorbance is detected at a wavelength of 880 nm. A correction to all seawater samples is made for the refractive index between seawater and the deionized water baseline. TDP samples, especially those with high SRP : DOP ratios, must be calibrated with standard solutions that have also been UV irradiated because slopes of the SRP vs. TDP calibration curves differ by ~1%, possibly because of the oxidizing matrix of the TDP samples. Ignoring this step could lead to errors in deep-ocean DOP values of 50% or more. This method has a limit of quantification of ~30 nmol L^{-1} SRP and an average repeatability of 0.2%. Accuracy is determined by daily measurements of the Wako CSK standard phosphate solution at 0.5 μmol L^{-1} P (Wako #034-10011); over the course of this study, we obtained an average value of 0.492 ± 0.008 (1σ) μmol L^{-1} P. Colorimetric interference on SRP from silicate using sodium hexafluorosilicate is negligible at Si concentrations below 70 μmol L^{-1} and at higher concentrations is 0.14 nmol L^{-1} "apparent" SRP per 1 μmol L^{-1} Si. In quartz dissolution experiments, however, we have found a greater interference, 0.5 nmol L^{-1} SRP per 1 μmol L^{-1} Si, presumably because of differences in Si speciation. By acidifying TDP samples to pH ~6 in the quartz UV vials (which slows the dissolution kinetics for SiO_2; Mazer and Walther 1994) and cooling the UV sample chamber (*see* Sample Handling section), the in-growth of quartz-derived silicate is only 2–3 μmol L^{-1}, meaning an interference of <2 nmol L^{-1} SRP in any given TDP sample. TDP and SRP for each sample are analyzed back-to-back in triplicate and DOP is calculated as (TDP − SRP). In interpreting SRP as "inorganic," it is important to consider that some of the measured SRP may not be PO_4^{3-}, but acid-hydrolyzed DOP, which is known to occur in the molybdenum blue protocol (Weil-Malherbe and Green 1951; Rigler 1968). Running solutions of organic compounds with our analytical setup, we observed 0% acid hydrolysis of some compounds (such as DNA) and up to 8% of other compounds (such as calcium glycerophosphate). Interestingly, the apparent acid hydrolysis seemed to scale with the stated purity of the starting reagents, so it is difficult to rule out reagent contamination. In any case, interpreting SRP as inorganic P yields a lower bound for DOP concentrations.

As a comparison to UV oxidation, TDP was also determined by wet persulfate oxidation (PS-ox) following the procedure of Menzel and Corwin (1965). Seawater samples (40 mL in triplicate) were amended with 5 mL of a 6.4% potassium persulfate solution and autoclaved (121°C) for 40 min. The oxidized samples were concentrated by MAGIC (Karl and Tien 1992) and then analyzed using standard colorimetric methods (Murphy and Riley 1962) on a DU640 spectrophotometer at 880 nm using a 10 cm path-length cell. Blanks were made from artificial seawater (Instant Ocean) from which inorganic P was removed by MAGIC. Standards and blanks were treated in the same way as the samples.

DOC concentrations were determined by a HTC method performed on a modified Shimadzu TOC-V as described by Carlson et al. (2010). Briefly, CO_2-free carrier gas was produced with a Balston gas generator providing a flow rate of 168 mL min^{-1} for analyses. Samples were drawn into a 5 mL injection syringe, acidified with 2 mol L^{-1} HCl (1.5%), and sparged (100 mL min^{-1}) for 1.5 min with CO_2-free gas, producing sample containing only nonpurgeable organic carbon. Three to five replicates of 100 μL of the resulting sample were injected into a combustion tube heated to 680°C, where the organic carbon was oxidized to CO_2. The resulting CO_2 and carrier gas were passed through an electronic dehumidifier, a magnesium perchlorate water trap, a copper mesh halide trap, and 0.2 μm filter and then analyzed by the nondispersive infrared gas analyzer. The resulting peak area was integrated with Shimadzu chromatographic software. For every HTC DOC sample analysis, calibration was achieved using glucose solutions (25–100 μmol L^{-1} C) in nanopure deionized water. For quality assurance, all samples were systematically referenced against internal reference waters every 6–8 samples, and accuracy was confirmed using consensus reference material (natural seawater with 38–80 μmol L^{-1} C) provided by D. Hansell's Organic Biogeochemistry Laboratory at the University of Miami (Hansell 2005). The precision for DOC analysis is ~1 μmol L^{-1} or a CV of 2–3%.

Field samples

Seawater samples were collected at or near Station ALOHA, located 100 km north of Oahu, Hawaii, at 22°45′N, 158°00′W, during various cruises from 2016 to 2017 (*see* Supporting

Information). Seawater was collected using a CTD rosette of 24 twelve-liter Bullister bottles. Samples collected for inorganic nutrients, UV photo-oxidation, and PS-ox were immediately dispensed into 250 or 500 mL bottles (either polypropylene or high-density polyethylene) and stored in a −20°C freezer (Dore et al. 1996). Prior to analysis, samples were thawed overnight in a refrigerator then brought to room temperature. Samples for TDN and DOC analysis by HTC were collected in a separate bottle and then either (1) immediately acidified using 1.5 mL of 4 mol L^{-1} HCl per liter of seawater and stored in a refrigerator until analysis or (2) frozen like the nutrient samples.

All seawater samples are unfiltered in order to have the lowest possible risk of contamination through handling, which is only justified in this case because the abundance of C-, N-, and P-bearing particulates is very low. Particulate C at Station ALOHA is 1.5–3 μmol L^{-1} in the mixed layer and <1 μmol L^{-1} below 250 m depth; particulate N is 0.2–0.4 μmol L^{-1} in the mixed layer and drops to <0.1 μmol L^{-1} below 250 m depth; and particulate P is generally 10–20 nmol L^{-1} in the mixed layer and <4 nmol L^{-1} below 250 m depth (Karl et al. 2001; Hebel and Karl 2001; also see depth profiles in the Supporting Information). In summary, the possible contribution from particulates to our DOC, DON, and DOP values is less than or equal to the limit of our analytical precision for waters deeper than 250 m (*see* Table 2 as well as the section above on Analytical Methods). It is for this reason, combined with our focus on deep water, that we do not use the terms total organic C, N, and P (TOC, TON, and TOP) in the difference calculation. When working in shallow water or other locations with a higher particulate load, it becomes necessary and proper to consider that—in unfiltered samples—DON (for example) is truly (TDN – [N + N] – NH_4^+ – particulate N).

Table 2. Reproducibility of N + N, TDN, DON, and TDP of natural seawater samples from Station ALOHA. HOT 288 is Hawaii Ocean Time-series cruise 288 (November 2016). KOK1703 samples were taken from cruise 1703 (March 2017) of the R/V Ka`imikai-O-Kanaloa.

Sample	Depth (m)	Conc. (μmol L^{-1})	1σ (μmol L^{-1})	No. days
TDN				
HOT 288 SSW*	1	4.95	0.09	15
KOK1703-2-7-22*	5	4.80	0.09	15
KOK1703-2-7-1	300	9.28	0.08	5
KOK1703-2-5-11	500	36.41	0.18	5
KOK1703-2-5-1	1000	45.06	0.18	4
N + N				
KOK1703-2-7-1	300	5.70	0.10	5
KOK1703-2-5-11	500	33.40	0.20	5
KOK1703-2-5-1	1000	42.51	0.26	4
DON				
KOK1703-2-7-1	300	3.57	0.05	5
KOK1703-2-5-11	500	3.00	0.12	5
KOK1703-2-5-1	1000	2.46	0.15	4
TDP				
HOT 288 SSW*	1	0.245	0.004	14

SSW, surface seawater.
*N + N and SRP concentrations are <10 nmol L^{-1} and ~60 nmol L^{-1}, respectively.

High-molecular-weight DOM

To test the recovery of DON and DOP from natural material, high-molecular-weight (HMW) DOM was obtained by ultrafiltration of surface seawater (SSW), which was collected offshore of the Natural Energy Laboratory of Hawaii Authority on the Island of Hawaii, following the procedure described in Repeta and Aluwihare (2006) with an added step to remove residual humic substances using anion exchange resin (Repeta et al. 2016). This HMW DOM fraction includes compounds with nominal weights of 1–30 kDa and represents ~30% of the total DOC (Zigah et al. 2017). With respect to its DON and DOP, it is dominated in composition by amide N, as occurs within peptide bonds and N-acetyl sugars (Aluwihare and Meador 2008), and P-bearing polysaccharides (Repeta et al. 2016). The N content of the HMW DOM powder was determined by combustion on an Exeter Analytical CE-440 Elemental Analyzer. The P content was determined using the high-temperature filter combustion method of Karl et al. (1991) by wetting glass fiber filters with a stock solution prepared from the HMW DOM powder.

Results and discussion

Irradiance times and method precision

Time series irradiations of SSW from Station ALOHA were performed in order to determine the exposure times required for maximum yields of DON and DOP. As previously found (Armstrong et al. 1966), the DOP portion of DOM is oxidized faster than DON with 95% of DOP being recovered within 45 min of irradiation, whereas 97% of DON is recovered within 4 h (Fig. 1).

Photo-oxidation occurs through a set of highly complex chain reactions; for example, the complete mineralization of ethanol is accomplished through 40 unique reactions (Oppenländer 2003). Therefore, it is somewhat surprising to find that oxidation of natural samples can be approximated with first-order, exponential decay kinetics for at least the first ~95% of mineralization; for the last ~5%, our method is not precise enough to resolve the decay kinetics for this system. Decay constants can be calculated with a linear regression of the exponential decay equation,

$$\ln\left(\frac{\mathrm{DON_f}}{\mathrm{DON_f} - \mathrm{DON_t}}\right) = \lambda t \quad (1)$$

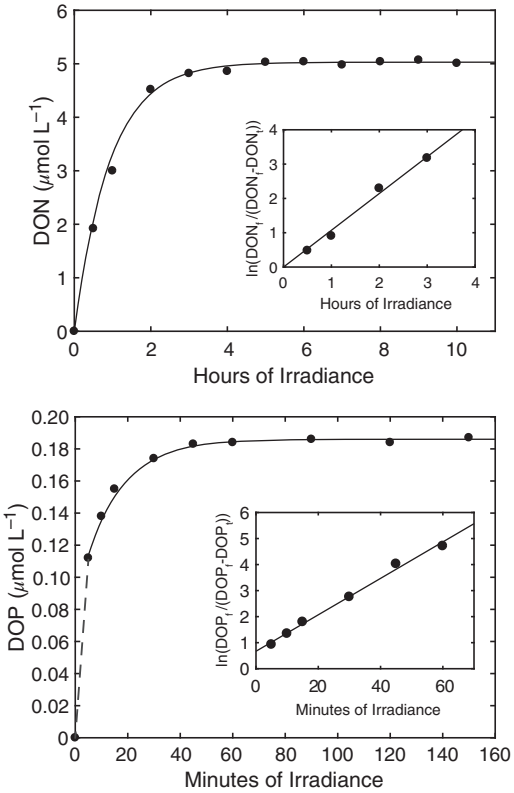

Fig. 1. Time series irradiation of SSW from Station ALOHA for DON (top panel) and DOP (bottom panel). Inset plots are fits of the exponential decay equation (Eq. 1; *see* text) and are used to plot the decay curves for DON and DOP. The dashed line in the DOP plot indicates the higher decay rate of DOP during the first 5 min of irradiance.

where λ is the decay constant (h^{-1}) and DON_f and DON_t are obtained as N+N (μmol L^{-1}) measurements after the maximum irradiation time and at time, *t* (h), respectively. Using data from the first 3 h of oxidation yields a decay constant of 1.1 h^{-1} for DON in SSW (Fig. 1) and 1.4 h^{-1} for L-arginine (data not shown), translating to half-lives of 0.65 and 0.51 h, respectively. Selecting an irradiation time of 8 h for a DON digestion therefore represents 12 half-lives. Using Eq. 1 for DOP, we find that the decay constant for DOP in SSW is 9 min (Fig. 1); therefore, there are 10 half-lives in our 90 min digestion. Unlike DON, the regression through DOP points is poor if the intercept is forced to zero (as it theoretically should be) and interpreted to mean that oxidation of DOP is especially rapid in the first 5 min of irradiation and then slows to the 9 min half-life.

Table 2 shows the reproducibility of natural samples for TDN and TDP colorimetric determinations made over many days using the oxidation times of 8 h and 90 min, respectively, along with N+N and DON. The reproducibility of TDN and TDP is equivalent to that of our Wako CSK reference standards (*see* Analytical Methods section), suggesting that the UV oxidation step introduces less variability than the colorimetric analysis itself. The reproducibility of DON is better than expected based on the error propagation of N+N and TDN. For example, using the 1000 m deep sample from Table 2, the reproducibility of DON is predicted to be ± 0.31 μmol L^{-1}, but we found half as much variability. This is a clear illustration of why it is important to analyze the oxidation products of TDN (or TDP) samples in the same analytical run with N+N (or SRP), especially those with low organics; errors are lower because they depend on repeatability and not daily variations in accuracy.

Recovery of model compounds

A traditional way to determine oxidation efficiency/completion is by the extent to which known organic compounds can be recovered in the form of their mineralized oxidation products, in this case, N+N and SRP. Therefore, we tested various common, naturally occurring DON and DOP compounds for procedural N+N and SRP recovery. Unless noted, all solutions were prepared in Station ALOHA SSW. Unspiked SSW was run with every batch of prepared solutions so that background TDN and TDP could be subtracted from the spiked solutions in the calculation of percent recovery; this explicitly assumes that background DOM oxidizes to the same extent in spiked and unspiked solutions. Although it may be more straightforward to use deionized water, a number of reports have shown unpredictably different recoveries between seawater and deionized water solutions (Kérouel and Aminot 1996; Bronk et al. 2000), indicating that testing the proper matrix is crucial. An additional point of importance is that, until now, no studies have reported DON and DOP oxidation recoveries from natural marine DOM, leaving one to wonder whether or not the oxidation behavior of single compounds applies to field samples.

Recoveries for DON and DOP are shown in Table 3. The recoveries of DON are similar to some of the highest values previously reported by Walsh (1989) and in the compilation by Bronk et al. (2000). For 11 different compounds, recovery is highly repeatable, insensitive to concentration, and ranges from 86% to 100%—with the exception of urea, which is known to be resistant to UV photo-oxidation (Armstrong et al. 1966; Walsh 1989). Urea is a special case that shows variable recovery (47–77%) depending on concentration, whether or not other compounds are added (for example, one of the higher recoveries, 62%, was obtained when glycine was added to the urea solution) and irradiance times are extended beyond the normal 8 h. These observations make it difficult to predict how UV oxidation of urea proceeds in natural samples, but its low concentration in most settings (Sipler and Bronk 2015) means it will not greatly influence DON estimates. Conversely, natural HMW DOM is efficiently oxidized (DON recovery is 98%) and it represents a much more significant portion of DON in natural waters. Omitting urea, the average DON recovery from known compounds is 94%. No ammonium was detected as a mineralization product (<10 nmol L^{-1}) using the high-sensitivity protocol from Holmes et al. (1999).

Table 3. Recovery of DON and DOP from various compounds following UV oxidation. All solutions were prepared in SSW from Station ALOHA. Concentration is expressed as DON and DOP, not concentration of the compound.

Compound	Conc. (μmol L^{-1})	Recovery (%)	1σ (%)	*n*
Nitrogen				
Adenosine	5 and 10	87%	0.7%	6
Adenosine triphosphate	5 and 10	86%	0.9%	6
Ammonium sulfate	5 and 10	98%	0.5%	6
Bovine serum albumin*	5 and 10	94%	2.0%	5
DNA sodium salt*	5 and 10	87%	1.2%	6
EDTA	5 and 10	99%	1.1%	6
Glucosamine	5 and 10	99%	0.6%	5
Glycine	5 and 10	100%	1.1%	9
HMW DOM*	3, 5, 16, and 27	98%	0.8%	12
L-arginine	5 and 10	93%	1.1%	12
Urea	1, 5, and 10	47–77%		23
Phosphorus				
Monomeric P compounds				
Adenosine monophosphate	1	76.0%	0.2%	6
DNA sodium salt†	1.2	99.8%	0.2%	6
Glucose-6-P	1	97.7%	0.4%	6
Glycerophosphate	1	94.4%	0.3%	6
HMW DOM†	0.3	99.2%	2.6%	4
Methylphosphonate	1	91.6%	1.2%	6
Polyphosphates				
Adenosine triphosphate	1	7.6%	0.5%	6
Pyrophosphate	1	1.1%	0.3%	6
Tripolyphosphate	1	1.6%	0.8%	5

*Nitrogen content of starting powder was determined by combustion on an Exeter Analytical CE-440 Elemental Analyzer.
†Phosphorus content of starting material was determined by the high-temperature filter combustion method of Karl et al. (1991).

The UV oxidation of DOP is highly selective for monomeric P compounds, with an average recovery of 93% (Table 3). The nearly negligible recovery of polyphosphates (PPs) is within error of the SRP values obtained by analyzing the solutions before UV irradiation, suggesting that any "UV recovery" is actually acid hydrolysis during colorimetric detection (e.g., Thomson-Bulldis and Karl 1998), phosphate contamination of the starting reagents, or due to larger errors near our limit of detection. If PPs do occur in marine TDP, the total P budget will be underestimated by UV oxidation; however, if there are only inorganic PPs (albeit these can be biogenic), DOP estimates will be accurate. Enzymatic hydrolysis of organic PPs occurs in natural waters, which explains why the concentration of dissolved adenosine triphosphate (ATP), for example, is very low (<1 nmol L^{-1} ATP; Björkman and Karl 2001, 2005); however, it is not known if all organic PPs are affected to the same extent. Repeta et al. (2016) recently used phosphorus-31 nuclear magnetic resonance to identify P functional groups in HMW DOM collected from Station ALOHA and determined that pyrophosphate comprises 6% of its total P; however, we recovered 99% of the P from HMW DOM, suggesting the absence (or a very low percentage) of pyrophosphate. Another way to test for PPs in natural waters is to compare TDP values obtained with UV oxidation to those using PS-ox as PS-ox has been shown to fully recover PPs (Thomson-Bulldis and Karl 1998). Theoretically, the difference between the two methods could be an estimate for PPs abundances, although low abundances could be below analytical precision, and, based on our method comparison (*see* below), there are other undefined complications. A possible analytical solution for obtaining the highest possible recovery of DOP may be a combined UV plus PS-ox technique (e.g., Ridal and Moore 1990), but reagent blanks would complicate its application to low-level DOP work such as in the deep oceans.

Method comparison for TDN

HTC typically results in better recoveries of known, nitrogenous organic compounds than does UV oxidation, with HTC showing yields of ~95–105% N and UV oxidation almost always returning yields <100% and as low as ~50% (Armstrong et al. 1966; Walsh 1989; Collos and Mornet 1993; Bronk et al. 2000; this study). Natural seawater samples are another matter, with some studies showing no significant difference between methods (Walsh 1989; Sharp et al. 2002) and others showing a clear deficiency in TDN obtained through UV oxidation (Bronk et al. 2000). Here, we compare our UV method to the HTC method using 49 seawater samples spanning a concentration range of 5–45 μmol L^{-1}N (Fig. 2). The slope of a reduced major axis regression, fit through the comparison plot, is 1.004 ± 0.009 (1σ) and the average ratio of TDN_{UV}/TDN_{HTC} is

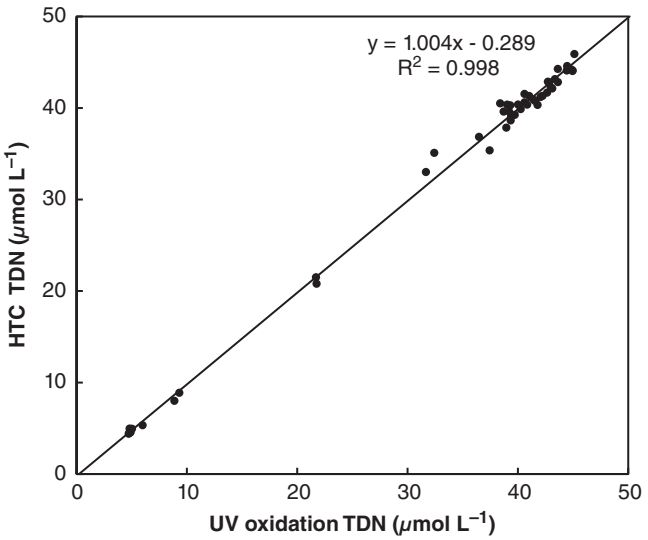

Fig. 2. Comparison of TDN values obtained by UV oxidation to those obtained through HTC; all samples are natural seawater obtained at or near Station ALOHA (*n* = 49).

1.01 ± 0.04 (1σ); there is no apparent offset or bias between methods. This finding is strong evidence that our UV oxidation efficiency for natural seawater samples is equal to what are arguably the most aggressive oxidation conditions available and that recovery of model compounds does not accurately predict the behavior of natural seawater.

Method comparison for TDP

Most P-bearing compounds, including PPs, are recovered to a high degree using PS-ox followed by colorimetric detection of SRP (Menzel and Corwin 1965; Kérouel and Aminot 1996; Thomson-Bulldis and Karl, 1998). *A priori*, one would then expect UV oxidation to underestimate the DOP found by PS-ox by at least the amount present as PPs. But in fact, we found an average of 15% higher DOP using UV oxidation than PS-ox for samples of the upper water column at Station ALOHA (0–200 m; Fig. 3). Interestingly, PS-ox only yields the same (within error) or more than UV oxidation at depths that are 10 to 40 m below the deep chlorophyll maximum (~110 m), hinting at possible changes in speciation or the general character of DOM. Ridal and Moore (1990) also found UV oxidation to yield slightly higher TDP for seawater samples than PS-ox, although both methods gave lower results than a modified, combination method. An empirical study by Karl and Yanagi (1997) found that in the upper 100 m at Station ALOHA, a greater portion of DOP was oxidized by low-intensity UV light than DOP deeper than 100 m, which also supports the notion of a depth-dependent change in the speciation of organic compounds and hence a change in how different oxidation methods may compare.

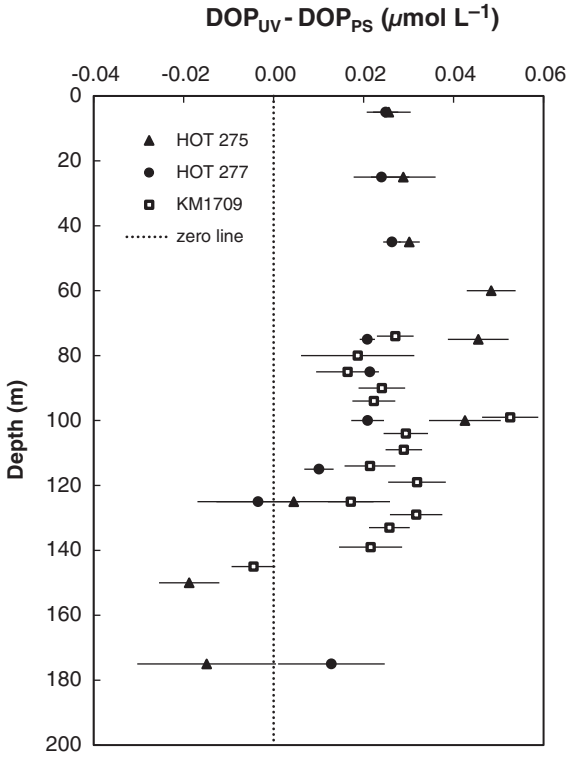

Fig. 3. Plot showing the difference between DOP values obtained using our UV oxidation method and DOP values obtained through PS-ox for seawater samples collected from the upper water column of Station ALOHA during HOT cruises 275 and 277 as well as cruise #1709 aboard the R/V *Kilo Moana*. Error bars are propagated errors of analytical uncertainty (1σ). The TDP of these samples ranges from 0.21 to 0.48 μmol L^{-1}, and DOP ranges from 0.07 to 0.21 μmol L^{-1}.

Similar to our findings for DON recovery, we find that model compounds behave differently during oxidation than molecular assemblages of natural seawater, and it could be misleading to assume the known compounds are truly representative. This is somewhat unsettling because it deprives these oxidation methods of a true benchmark of performance and highlights the acute need for a natural reference material for DOP and DON analyses.

Station ALOHA water column profiles

Full ocean depth profiles (5–4800 m) of TDN, N + N, TDP, and SRP, along with resulting values for DON and DOP, are shown in Fig. 4 for seawater samples from Station ALOHA in the North Pacific Subtropical Gyre (*see* Supporting Information for data and cruise information). Because DON values are based on duplicate TDN/N + N measurements, it is difficult to assign error estimates to individual DON values. Instead, we assign errors based on the reproducibility of DON as shown in Table 3, which averages ± 0.1 μmol L^{-1} (1σ) over the whole concentration range of TDN. Error estimates of individual DOP values, however, are based on the propagation of repeatability for triplicate TDP/SRP sets and averages ± 0.004 μmol L^{-1} (1σ) over the whole concentration range of TDP (*see* Supporting Information). Samples for N analyses were obtained from five different cruises, but samples for P analyses were from a single cruise (HOT 293). Note again that these field samples were not filtered in order to avoid contamination through handling; particulate C, N, and P concentrations are above analytical error only in the shallowest samples (5–250 m depth), so it is more accurate to refer to these shallow data points as TOC, TON, and TOP.

All parameters for the upper 900 m conform well to the established climatology for Station ALOHA (*see* Karl et al. 2001). Below 900 m, there is limited published data with which to compare the DON and DOP data of this study, and what are available are universally more variable (Table 4). Unlike the concentration of inorganic nutrients, no gradient in DON or DOP is observed in the 900–4800 m depth range. Our average DON value for below 900 m is 2.24 ± 0.15 μmol L^{-1} (1σ, $n = 49$) or 5–6% of TDN. This DON value is similar to that reported by Karl et al. (2001) or Loh and Bauer (2000), but we show significantly less variability and greater depth resolution. Using our TDN data obtained through HTC (data shown in Fig. 2), DON for depths below 900 m is 2.15 ± 0.83 μmol L^{-1} (1σ, $n = 23$), a similar average but with over five times the variability. Previous estimates for DOP in deep Pacific waters vary by an order

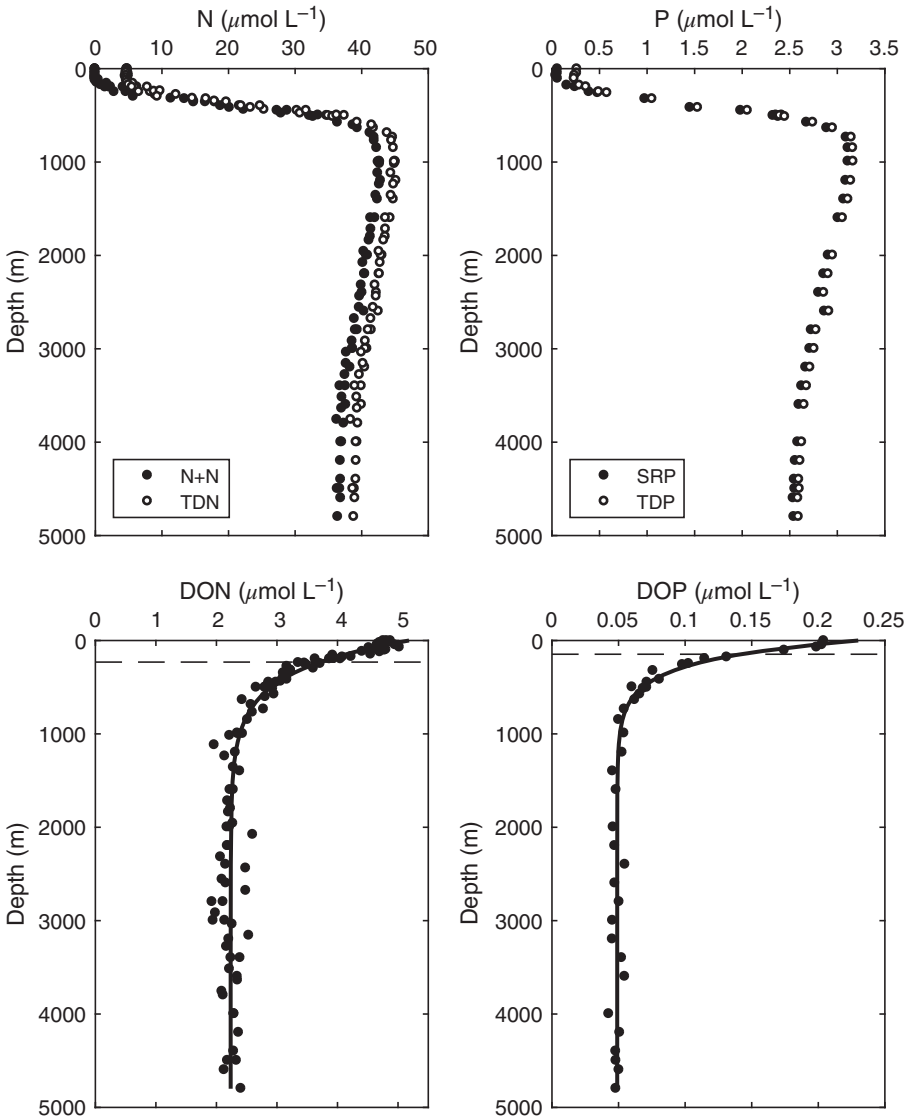

Fig. 4. TDN, N + N, TDP, SRP, DON, and DOP profiles for seawater in the vicinity of Station ALOHA. Model curves for DON and DOP are based on Eq. 2 (*see* text), and fit parameters are reported in Table 5. Dashed lines on the bottom panels represent "half-life depth" and are 231 and 151 m for DON and DOP, respectively.

of magnitude, from 0.016 to >0.2 μmol L^{-1} (Table 4), but we obtain an average deep-water DOP in the narrow range of 0.049 ± 0.004 μmol L^{-1} (1σ, $n = 19$), which amounts to <2% of TDP.

The TDN : TDP ratio in samples above 400 m ranges from 15.8 to 18.4 and below 400 m averages 14.7 ± 0.3 (*see* Supporting Information); these values are consistent with the 9-yr observation period at Station ALOHA presented by Karl et al. (2001). DON : DOP ratios, however, are much higher, ranging from 24 at the surface and increasing to an average of 45 ± 4 for depths greater than 400 m (Fig. 5). Significant systematic changes in the DOC : DON ratio with depth are not observed in this dataset, with the possible exception of slightly lower values in the upper water column (~14 above 750 m and an average of 16.4 ± 1.3 below 750 m). Similar trends were observed in the Sargasso Sea where the lowest DOC : DON ratios occurred in the upper 500 m (~13.5), although maximum values in deep water showed an increase to only 14.5 (Hansell and Carlson 2001). DOC : DOP ratios in our Station ALOHA profiles, conversely, show a steep gradient in the upper 1000 m, starting at a ratio of 350 in the surface and more than doubling at depth (Fig. 5).

Implications for marine DOM

A simplified model of marine DOM is as follows: refractory DOM is uniformly distributed throughout the ocean, new DOM (often termed labile and semilabile, or more simply as bioavailable) is primarily created in the euphotic zone, and

Table 4. Various estimates for DON and DOP in deep ocean water (≥900 m) of the North Pacific Ocean.

Reference	Location and depth range	Average (μmol L^{-1}) $\pm$ 1σ (% CV)	Oxidation method	*n*
DON				
Williams et al. (1980)	Central N Pacific, 1000–5680 m	4.0 $\pm$ 0.4 (10%)	UV	5
Loh and Bauer (2000)	Eastern North Pacific, 1282–4097 m	2.38 $\pm$ 0.4 (16%)	PS-ox	5
Karl et al. (2001)	Station ALOHA, 900–1200 m	2.09 $\pm$ 0.5 (25%)	UV	200
This study	Station ALOHA, 900–4800 m	2.24 $\pm$ 0.15 (7%)	UV	49
DOP				
Williams et al. (1980)	Central North Pacific, 1000–5680 m	0.202 $\pm$ 0.036 (18%)	UV	5
Ridal and Moore (1992)	NE Subarctic Pacific, 1200–3800 m	0.02 $\pm$ 0.01 (50%)	UV plus persulfate	5
Thomson-Bulldis and Karl (1998)	Station ALOHA, 1000–4500 m	0.016 $\pm$ 0.012 (75%)	Modified persulfate*	18
Loh and Bauer (2000)	Eastern N Pacific, 1282–4097 m	0.088 $\pm$ 0.011 (13%)	High temperature ashing†	5
Karl et al. (2001)	Station ALOHA, 900–1050 m	0.030 $\pm$ 0.023 (77%)	UV	195
This study	Station ALOHA, 900–4800 m	0.049 $\pm$ 0.004 (8%)	UV	19

*Method that attempts to measure DOP directly by PS-ox of supernatants following the removal of inorganic phosphate by the MAGIC technique of Karl and Tien (1992)
†Solórzano and Sharp (1980) protocol

Table 5. Model fit parameters for DON, DOP, and DOC profiles at Station ALOHA using Eqs. 2 and 3 from the text. DON and DOP model fits are based on data presented here. The DOC model fit is based on data from the HOT database; see text for details.

Component	*a* (μmol L^{-1})	*b* (m^{-1})	*c* (μmol L^{-1})	R^2	"Half-life" depth (m)
DON	2.94	−0.0030	2.24	0.96	231
DOP	0.18	−0.0046	0.049	0.98	151
DOC	41.65	−0.0038	37.93	0.92	182

biological degradation and remineralization of DOM (primarily by bacteria) occurs progressively with depth and time (Carlson 2002; Hansell et al. 2012; Carlson and Hansell 2015). With this world view in mind, the DON and DOP full ocean depth profiles were fit using an exponential decay equation of the following form,

$$\mathrm{DON\,(or\,DOP)} = a \times e^{\mathrm{depth}\cdot b} + c \quad (2)$$

where a is the concentration (μmol L^{-1}) of bioavailable DON (or DOP), b (m^{-1}) is the decay constant for bioavailable material with respect to ocean depth (m), and c is the concentration (μmol L^{-1}) of refractory DON (or DOP). Fit parameters are listed in Table 5. The half-life of bioavailable DON (or DOP) with depth (i.e., the depth at which half of the bioavailable material is remineralized) is calculated as,

$$\mathrm{depth}_{1/2} = -\frac{\ln 2}{b} \quad (3)$$

From the model curves in Fig. 4, the half-life depth of DON is 231 m and for DOP is shallower at 151 m, indicating, as others have observed (Clark et al. 1998; Loh and Bauer 2000; Aminot and Kérouel 2004; Letscher and Moore 2015), that P is preferentially remineralized over both N and C in the epipelagic zone. Severe and preferential P depletion in deep-sea DOM is also reinforced by the two-fold gradient of DOC : DOP over the 0–1000 m depth range, where DOC : DON is comparatively invariant. Note that the concentration of particulate N and P (with paired analyses) would result in the next level of refinement of these curves within the upper 250 m, but based on historical data, it would result in relatively small adjustments.

The fit parameters for DOC that are listed in Table 5 are derived from the HOT database (available at http://hahana.soest.hawaii.edu/hot/hot-dogs/) and allow us to construct model profiles of DOC : DON and DOC : DOP (Fig. 5), yielding a deep-sea DOC : DON : DOP molar stoichiometry of 759 : 45 : 1. Preliminary estimates for the global ocean budget of refractory DON and DOP (RDON and RDOP) were calculated by applying this deep-sea stoichiometric relationship to the global inventory of refractory DOC (RDOC, 630 Pg; Hansell 2013) and found to be 43.6 Pg N and 2.14 Pg P, respectively. This is over four times more P than would be calculated if using the stoichiometric relationship of global RDOM estimated by Hopkinson and Vallino (2005) (DOC : DON : DOP = 3511 : 202 : 1), which in part derives from Station ALOHA data. We argue that this discrepancy is due to previous analytical difficulties in measuring DOP concentrations in waters with high SRP : DOP ratios. Verifying the stoichiometry of deep DOM to high

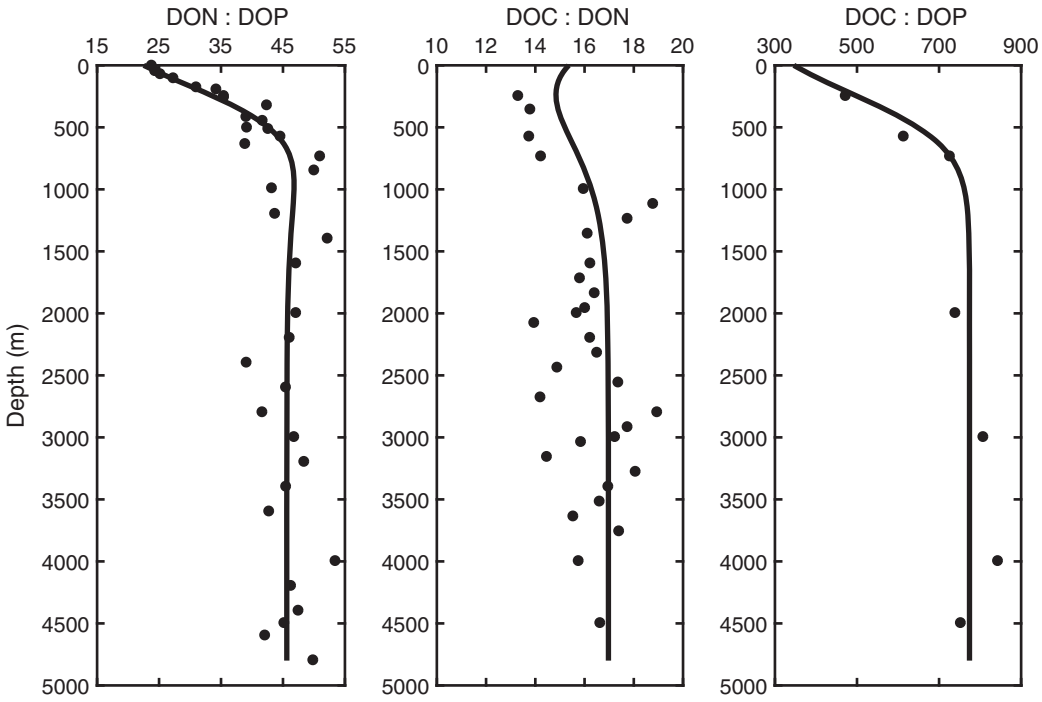

Fig. 5. Stoichiometric ratios of N, P, and C in DOM at Station ALOHA. Curves are based on the model parameters reported in Table 5 (details in text). Individual points are data from this study and are available in the Supporting Information. For depths greater than ~1500 m, the DOC : DON : DOP molar ratio is 759 : 45 : 1.

precision in other ocean basins will lead to more substantiated estimates of RDOM's elemental inventories. Although the refractory inventory of DOM contains 95% of marine DOC (Hansell 2013), we predict that globally it will harbor a lower percentage of the total P budget than N and C because DOP is highly depleted in deep water with respect to the other elements. From our profiles, the abundance of bioavailable DOP is 15% of the total depth-integrated DOP (0–4800 m; 0.28 mol m^{-2}), whereas bioavailable DON is only 8% of the total depth-integrated DON (0–4800 m; 11.74 mol m^{-2}).

Despite the good model fits in Fig. 4, they might only be a descriptive tool (e.g., to compare ocean basins or environmental settings), as there are many lines of evidence illustrating that the biogeochemical character of marine DOM is much more nuanced, much more dynamic and that there is a complicated layering of many biological and chemical processes occurring over many temporal and spatial scales (*see* reviews by Karl [2014], Repeta [2015], Carlson and Hansell [2015], and Dittmar [2015]). Ultimately, the fundamental question with regard to deep-sea DOM is: with >200 times more reduced carbon than all of marine biomass (Hansell et al. 2009), why is it not fueling abundant biological growth in the deep ocean? The ~4000–6000 year old radiocarbon age of bulk DOM in deep ocean water (Druffel et al. 1992) has generally been regarded as rational for its "refractory" label; however, it is younger than the Earth's last glacial period and by no means inert. If it is not bioavailable, then why is it only ~4000–6000 yr old and why is there only ~40 μmol L^{-1} of DOC? It is possible that the DOM compounds are configured in such a way that they resist rapid biological degradation (Benner and Amon 2015) and that heat or energy is the "limiting nutrient" of biological activity at depth (Church 2008), causing DOM turnover times to be slow. Alternatively, the "molecular diversity" hypothesis (Kattner et al. 2011; Dittmar 2015) states that any given organic compound in the myriad of DOM compounds is at such low concentration that it simply escapes microbial detection and the sum total of these diverse compounds are comparable to what is considered RDOM. Arrieta et al. (2015) conducted experiments adding concentrated deep-sea DOM to natural prokaryotic assemblages from 1000 to 4200 m deep water of the Pacific Ocean and found a strong relationship between DOC concentration and specific growth rates, ultimately rejecting the paradigm of recalcitrance as an explanation for the large pool of refractory marine DOM. In any case, with a limited biological sink, other abiotic sinks must be more accurately quantified. Repeta (2015) and Carlson and Hansell (2015) review some important DOM removal processes, all of which need better constraints in terms of both elemental fluxes and spatial distribution: stripping of DOM via hydrothermal circulation at mid-ocean ridges; adsorption of DOM onto sinking particles; condensation of microgels from HMW DOM; and photochemical oxidation or transformation of DOM when it circulates through the euphotic zone.

The amassed knowledge is revealing an intimidating truth: every single compound in the conglomeration that is DOM has its own residence time, a unique origin, a unique bioavailability,

and a specific environmental setting in which it is most readily transformed, consumed, remineralized, or sequestered (whether that be biotically or abiotically). What is often missing from DOM studies are the N and P—the great majority of DOM work focuses on DOC. For example, there is a general trend in which molecular size of DOM is inversely correlated with radiocarbon age, essentially extending the size-reactivity continuum model from particulate organic matter down to the smallest dissolved organic molecules (Loh et al. 2004; Benner and Amon 2015; Walker et al. 2016*a*; Zigah et al. 2017). Recently, Walker et al. (2016*b*) demonstrated that C : N ratios also vary along the size-reactivity continuum for waters of the Pacific Ocean. We postulate that C : P ratios could show an even stronger signal as they are fractionated to a higher degree than C : N and are also highly sensitive to early mineralization within the photic zone. We are hopeful that introducing precise DON and DOP measurements into such topics will diversify discussions of DOM and help add dimension and understanding to the biogeochemical cycling of these essential elements.

Conclusions

We developed a high-precision UV photo-oxidation method for the determination of DON and DOP using a microwave-powered UV light system coupled to back-to-back colorimetric analyses of TDN with N+N and TDP with SRP. We observe no systematic offset between our UV method and the HTC method for TDN. We recover slightly higher TDP concentrations compared to the PS-ox method but only in seawater samples from <125 m deep. Reproducibility of DON and DOP averages ± 0.1 μmol L^{-1} (1σ) and ± 0.004 μmol L^{-1} (1σ), respectively, even at concentrations that are 5% of TDN and 2% of TDP. As a result, we are able to report the most well-constrained, full ocean depth profiles of DON and DOP available to date, using seawater samples from Station ALOHA in the North Pacific Subtropical Gyre. Deep-sea DOM (>1000 m deep) from our sample set has an average DON concentration of 2.24 ± 0.15 μmol L^{-1} (1σ, $n = 49$), an average DOP concentration of 0.049 ± 0.004 μmol L^{-1} (1σ, $n = 19$), and a DOC : DON : DOP stoichiometric relationship of 759 : 45 : 1, with no discernible gradients for any of these parameters in the 1000–4800 m depth range. We believe that, in the search for a greater understanding of sources, sinks, and overall biogeochemistry of DOM, many studies would benefit from having a precise method for evaluating N and P abundances in DOM.

References

Aluwihare, L. I., and T. Meador. 2008. Chemical composition of marine dissolved organic nitrogen, p. 95–140. *In* D. G. Capone, D. A. Bronk, M. Mulholland, and E. J. Carpenter [eds.], Nitrogen in the marine environment. Academic Press.

Aminot, A., and R. Kérouel. 2004. Dissolved organic carbon, nitrogen and phosphorus in the NE Atlantic and the NW Mediterranean with particular reference to non-refractory fractions and degradation. Deep-Sea Res. Part I. **51**: 1975–1999. doi:10.1016/j.dsr.2004.07.016

Armstrong, F. A., P. M. Williams, and J. D. H. Strickland. 1966. Photo-oxidation of organic matter in seawater by ultraviolet radiation, analytical and other applications. Nature **211**: 481–483. doi:10.1038/211481a0

Armstrong, F. A. J., and S. Tibbitts. 1968. Photochemical combustion of organic matter in sea water, for nitrogen, phosphorus and carbon determination. J. Mar. Biol. Assoc. UK **48**: 143–152. doi:10.1017/S0025315400032483

Arrieta, J. M., E. Mayol, R. L. Hansman, G. J. Herndl, T. Dittmar, and C. M. Duarte. 2015. Dilution limits dissolved organic carbon utilization in the deep ocean. Science **348**: 331–333. doi:10.1126/science.1258955

Beattie, J., C. Bricker, and D. Garvin. 1961. Photolytic determination of trace amounts of organic material in seawater. Anal. Chem. **33**: 1890–1892. doi:10.1021/ac50154a030

Benner, R., and R. M. W. Amon. 2015. The size-reactivity continuum of major bioelements in the ocean. Ann. Rev. Mar. Sci. **7**: 185–205. doi:10.1146/annurev-marine-010213-135126

Björkman, K., and D. M. Karl. 2001. A novel method for the measurement of dissolved adenosine and guanosine triphosphate in aquatic habitats: Applications to marine microbial ecology. J. Microbiol. Meth. **47**: 159–167. doi:10.1016/S0167-7012(01)00301-3

Björkman, K., and D. M. Karl. 2005. Presence of dissolved nucleotides in the North Pacific subtropical gyre and their role in cycling of dissolved organic phosphorus. Aquat. Microb. Ecol. **39**: 193–203. doi:10.3354/ame039193

Bronk, D. A., M. W. Lomas, P. M. Glibert, K. J. Schukert, and M. P. Sanderson. 2000. Total dissolved nitrogen analysis: Comparisons between the persulfate, UV and high temperature oxidation methods. Mar. Chem. **69**: 163–178. doi:10.1016/S0304-4203(99)00103-6

Carlson, C. A. 2002. Production and removal processes, p. 91–151. *In* D. Hansell and C. Carlson [eds.], Biogeochemistry of marine dissolved organic matter. Academic Press.

Carlson, C. A., D. A. Hansell, N. B. Nelson, D. A. Siegel, W. M. Smethie, S. Khatiwala, M. M. Meyers, and E. Halewood. 2010. Dissolved organic carbon export and subsequent remineralization in the mesopelagic and bathypelagic realms of the North Atlantic basin. Deep-Sea Res. Part II. **57**: 1433–1445. doi:10.1016/j.dsr2.2010.02.013

Carlson, C. A., and D. Hansell. 2015. DOM sources, sinks, reactivities and budgets, p. 65–126. *In* D. Hansell and C. Carlson [eds.], Biogeochemistry of marine dissolved organic matter, 2nd ed. Academic Press.

Church, M. J. 2008. Resource control of bacterial dynamics in the sea, p. 335–382. *In* D. L. Kirchman [ed.], Microbial ecology of the oceans, 2nd ed. Wiley-Liss.

Clark, L. L., E. D. Ingall, and R. Benner. 1998. Marine phosphorus is selectively remineralized. Nature **393**: 426–426. doi:10.1038/30881

Collos, Y., and F. Mornet. 1993. Automated procedure for determination of dissolved organic nitrogen and phosphorus in aquatic environments. Mar. Biol. **116**: 685–688. doi:10.1007/BF00355485

Curless, S. E., M. J. Church, M. Segura-Noguera, and D. M. Karl. 2017. Ammonium concentrations at Station ALOHA – Improved methodology allows for full ocean depth analysis. Abstract 29177 presented at ALSO Conference 2017, Honolulu, Hawaii.

Dittmar, T. 2015. Reasons behind the long-term stability of dissolved organic matter, p. 369–388. *In* D. Hansell and C. Carlson [eds.], Biogeochemistry of marine dissolved organic matter, 2nd ed. Academic Press.

Dore, J. E., T. Houlihan, D. V. Hebel, G. Tien, L. Tupas, and D. M. Karl. 1996. Freezing as a method of sample preservation for the analysis of dissolved inorganic nutrients in seawater. Mar. Chem. **53**: 173–185. doi:10.1016/0304-4203(96)00004-7

Druffel, E. R. M., P. M. Williams, J. E. Bauer, and J. R. Ertel. 1992. Cycling of dissolved and particulate organic matter in the open ocean. J. Geophys. Res. **97**: 15,639–15,659. doi:10.1029/92JC01511

Foreman, R. K., M. Segura-Noguera, and D. M. Karl. 2016. Validation of Ti(III) as a reducing agent in the chemiluminescent determination of nitrate and nitrite in seawater. Mar. Chem. **186**: 83–89. doi:10.1016/j.marchem.2016.08.003

Hansell, D. A. 2005. Dissolved organic carbon reference material program. EOS Trans. Am. Geophys. Union **86**: 318–319. doi:10.1029/2005EO350003

Hansell, D. A. 2013. Recalcitrant dissolved organic carbon fractions. Ann. Rev. Mar. Sci. **5**: 421–445. doi:10.1146/annurev-marine-120710-100757

Hansell, D. A., and C. A. Carlson. 1998. Deep-ocean gradients in the concentration of dissolved organic carbon. Nature **395**: 263–266. doi:10.1038/26200

Hansell, D. A., and C. A. Carlson. 2001. Biogeochemistry of total organic carbon and nitrogen in the Sargasso Sea: Control by convective overturn. Deep-Sea Res. Part II **48**: 1649–1667. doi:10.1016/S0967-0645(00)00153-3

Hansell, D. A., C. A. Carlson, D. J. Repeta, and R. Schlitzer. 2009. Dissolved organic matter in the ocean: A controversy stimulates new insights. Oceanography **22**: 202–211. doi:10.5670/oceanog.2009.109

Hansell, D. A., C. A. Carlson, and R. Schlitzer. 2012. Net removal of major marine dissolved organic carbon fractions in the subsurface ocean. Global Biogeochem. Cycles **26**: GB1016. doi:10.1029/2011GB004069

Hebel, D. V., and D. M. Karl. 2001. Seasonal, interannual and decadal variations in particulate matter concentrations and composition in the subtropical North Pacific Ocean. Deep-Sea Res. Part II **48**: 1669–1695. doi:10.1016/S0967-0645(00)00155-7

Holmes, R. M., A. Aminot, R. Kerouel, B. A. Hooker, and B. J. Peterson. 1999. A simple and precise method for measuring ammonium in marine and freshwater ecosystems. Can. J. Fish. Aquat. Sci. **56**: 1801–1808. doi:10.1139/f99-128

Hopkinson, C. S., and J. J. Vallino. 2005. Efficient export of carbon to the deep ocean through dissolved organic matter. Nature **433**: 142–145. doi:10.1038/nature03191

Karl, D. M. 2014. Microbially mediated transformations of phosphorus in the sea: New views of an old cycle. Ann. Rev. Mar. Sci. **6**: 279–337. doi:10.1146/annurev-marine-010213-135046

Karl, D. M., J. E. Dore, D. V. Hebel, and C. Winn. 1991. Procedures for particulate carbon, nitrogen, phosphorus and total mass analyses used in the US-JGOFS Hawaii Ocean Time-series program, p. 71–77. *In* D. C. Hurd and D. W. Spencer [eds.], Marine particles: Analysis and characterization. Geophysical Monograph 63. American Geophysical Union.

Karl, D. M., and G. Tien. 1992. MAGIC: A sensitive and precise method for measuring dissolved phosphorus in aquatic environments. Limnol. Oceanogr. **37**: 105–116. doi:10.4319/lo.1992.37.1.0105

Karl, D. M., and R. Lukas. 1996. The Hawaii Ocean Time-series (HOT) program: Background, rationale and field implementation. Deep-Sea Res. Part II. **43**: 129–156. doi:10.1016/0967-0645(96)00005-7

Karl, D. M., and K. Yanagi. 1997. Partial characterization of the dissolved organic phosphorus pool in the oligotrophic North Pacific Ocean. Limnol. Oceanogr. **42**: 1398–1405. doi:10.4319/lo.1997.42.6.1398

Karl, D. M., K. M. Björkman, J. E. Dore, L. Fujieki, D. V. Hebel, T. Houlihan, R. M. Letelier, and L. M. Tupas. 2001. Ecological nitrogen-to-phosphorus stoichiometry at station ALOHA. Deep-Sea Res. Part II **48**: 1529–1566. doi:10.1016/S0967-0645(00)00152-1

Karl, D. M., L. Beversdorf, K. M. Björkman, M. J. Church, A. Martinez, and E. F. Delong. 2008. Aerobic production of methane in the sea. Nat. Geosci. **1**: 473–478. doi:10.1038/ngeo234

Karl, D. M., and K. M. Björkman. 2015. Dynamics of DOP, p. 233–334. *In* D. Hansell and C. Carlson [eds.], Biogeochemistry of marine dissolved organic matter, 2nd ed. Academic Press.

Kattner, G., M. Simon, and B. P. Koch. 2011. Molecular characterization of dissolved organic matter and constraints for prokaryotic utilization, p. 60–61. *In* N. Jiao, F. Azam, and S. Sanders [eds.], Microbial carbon pump in the ocean. Science/AAAS.

Kérouel, R., and A. Aminot. 1996. Model compounds for the determination of organic and total phosphorus dissolved in natural waters. Anal. Chim. Acta **318**: 385–390. doi:10.1016/0003-2670(95)00461-0

Letscher, R. T., D. A. Hansell, C. A. Carlson, R. Lumpkin, and A. N. Knapp. 2013. Dissolved organic nitrogen in the global surface ocean: Distribution and fate. Global Biogeochem. Cycles **27**: 141–153. doi:10.1029/2012GB004449

Letscher, R. T., and J. K. Moore. 2015. Preferential remineralization of dissolved organic phosphorus and non-Redfield

DOM dynamics in the global ocean: Impacts on marine productivity, nitrogen fixation, and carbon export. Global Biogeochem. Cycles **29**: 325–340. doi:10.1002/2014GB004904

Loh, A. N., and J. E. Bauer. 2000. Distribution, partitioning and fluxes of dissolved and particulate organic C, N and P in the eastern North Pacific and Southern oceans. Deep-Sea Res. **47**: 2287–2316. doi:10.1016/S0967-0637(00)00027-3

Loh, A. N., J. E. Bauer, and E. R. M. Druffel. 2004. Variable ageing and storage of dissolved organic components in the open ocean. Nature **430**: 877–881. doi:10.1038/nature02780

Mazer, J. J., and J. V. Walther. 1994. Dissolution kinetics of silica glass as a function of pH between 40 and 85°C. J. Non-Crystal. Solids **170**: 32–45. doi:10.1016/0022-3093(94)90100-7

Menzel, A. F., and N. Corwin. 1965. The measurement of total phosphorus in seawater based on the liberation of organically bound fractions by persulfate oxidation. Limnol. Oceanogr. **10**: 280–282. doi:10.4319/lo.1965.10.2.0280

Moran, M. A. 2015. The global ocean microbiome. Science **350**: aac8455. doi:10.1126/science.aac8455

Murphy, J., and J. P. Riley. 1962. A modified single solution method for the determination of phosphate in natural waters. Anal. Chim. Acta **27**: 31–36. doi:10.1016/S0003-2670(00)88444-5

Oppenländer, T. 2003. Photochemical purification of water and air: Advanced oxidation processes (AOPs): Principles, reaction mechanisms, reactor concepts. Wiley-VCH.

Repeta, D. J. 2015. Chemical characterization and cycling of dissolved organic matter, p. 21–64. *In* D. Hansell and C. Carlson [eds.], Biogeochemistry of marine dissolved organic matter, 2nd ed. Academic Press.

Repeta, D. J., and L. I. Aluwihare. 2006. Radiocarbon analysis of neutral sugars in high-molecular-weight dissolved organic carbon: Implications for organic carbon cycling. Limnol. Oceanogr. **51**: 1045–1053. doi:10.4319/lo.2006.51.2.1045

Repeta, D. J., S. Ferrón, O. A. Sosa, C. G. Johnson, L. D. Repeta, M. Acker, E. F. DeLong, and D. M. Karl. 2016. Marine methane paradox explained by bacterial degradation of dissolved organic matter. Nat. Geosci. **9**: 884–887. doi:10.1038/ngeo2837

Ridal, J. J., and R. M. Moore. 1990. A re-examination of the measurement of dissolved organic phosphorus in seawater. Mar. Chem. **29**: 19–31. doi:10.1016/0304-4203(90)90003-U

Ridal, J. J., and R. M. Moore. 1992. Dissolved organic phosphorus concentrations in the northeast subarctic Pacific Ocean. Limnol. Oceanogr. **37**: 1067–1075. doi:10.4319/lo.1992.37.5.1067

Ridgewell, A., and S. Arndt. 2015. Why dissolved organics matter: DOC in ancient oceans and past climate change, p. 1–20. *In* D. Hansell and C. Carlson [eds.], Biogeochemistry of marine dissolved organic matter, 2nd ed. Academic Press.

Rigler, F. H. 1968. Further observations inconsistent with the hypothesis that the molybdenum blue method measures orthophosphate in lake water. Limnol. Oceanogr. **13**: 7–13. doi:10.4319/lo.1968.13.1.0007

Sharp, J. H., and others. 2002. A preliminary methods comparison for measurement of dissolved organic nitrogen in seawater. Mar. Chem. **78**: 171–184. doi:10.1016/S0304-4203(02)00020-8

Sipler, R. E., and D. A. Bronk. 2015. Dynamics of dissolved organic nitrogen, p. 127–232. *In* D. Hansell and C. Carlson [eds.], Biogeochemistry of marine dissolved organic matter, 2nd ed. Academic Press.

Solórzano, L., and J. H. Sharp. 1980. Determination of total dissolved phosphorus and particulate phosphorus in natural waters. Limnol. Oceanogr. **25**: 754–758. doi:10.4319/lo.1980.25.4.0754

Strickland, J. D. H., and T. R. Parsons. 1972. A practical handbook of seawater analysis. Bull. Fish. Res. Board Canada **167**: 71–80.

Thomson-Bulldis, A., and D. M. Karl. 1998. Application of a novel method for phosphorus determinations in the oligotrophic North Pacific Ocean. Limnol. Oceanogr. **43**: 1565–1577. doi:10.4319/lo.1998.43.7.1565

Torres-Valdés, S., and others. 2009. Distribution of dissolved organic nutrients and their effect on export production over the Atlantic Ocean. Global Biogeochem. Cycles **23**: GB4019. doi:10.1029/2008GB003389

Walker, B. D., F. W. Primeau, S. R. Beaupré, T. P. Guilderson, E. R. M. Druffel, and M. D. McCarthy. 2016a. Linked changes in marine dissolved organic carbon molecular size and radiocarbon age. Geophys. Res. Lett. **43**: 10,385–10,393. doi:10.1002/2016GL070359

Walker, B. D., S. R. Beaupré, T. P. Guilderson, M. D. McCarthy, and E. R. M. Druffel. 2016b. Pacific carbon cycling constrained by organic matter size, age and composition relationships. Nat. Geosci. **9**: 888–891. doi:10.1038/ngeo2830

Walsh, T. W. 1989. Total dissolved nitrogen in seawater: A new high temperature combustion method and a comparison with photo-oxidation. Mar. Chem. **26**: 295–311. doi:10.1016/0304-4203(89)90036-4

Weil-Malherbe, H., and R. H. Green. 1951. The catalytic effect of molybdate on the hydrolysis of organic phosphate bonds. Biochem. J. **49**: 286–292. doi:10.1042/bj0490286

Williams, P. M., A. F. Carlucci, and R. Olson. 1980. A deep profile of some biologically important properties in the central North Pacific gyre. Oceanol. Acta **3**: 471–476.

Zigah, P. K., A. P. McNichol, L. Xu, C. Johnson, C. Santinelli, D. M. Karl, and D. J. Repeta. 2017. Allochthonous sources and dynamic cycling of ocean dissolved organic carbon revealed by carbon isotopes. Geophys. Res. Lett. **44**: 2407–2415. doi:10.1002/2016GL071348

Acknowledgments

We are grateful for laboratory and/or intellectual support from the following people during the course of this study: Gabe Foreman, Oscar Sosa,

John Casey, Susan Curless, Carolina Funkey, Sam Wilson, Elisa Halewood, and Kendra Babcock. We thank Daniel Repeta for sharing his labor-intensive HMW DOM powder that was used for DON and DOP recovery testing. We also thank Steven Beaupré for advice on UV systems in the early stages of this project. Seawater samples were collected by the hard-working HOT and SCOPE field teams, especially Tara Clemente, Ryan Tabata, Tim Burrell, and Eric Shimabukuro, to all whom we owe much gratitude. This research was generously supported in part by the National Science Foundation (OCE-1260164 to D.M.K.), the Gordon and Betty Moore Foundation (grant 3794 to D.M.K.), the Simons Foundation (SCOPE award 329108 to D.M.K.), and a Simons Foundation International grant to C.A.C.

Conflict of Interest

None declared.

Submitted 10 September 2018
Revised 25 January 2019
Accepted 02 February 2019

Associate editor: Tammi Richardson

Improved UV photo-oxidation system yields estimates for deep sea dissolved organic nitrogen and phosphorus

Rhea K. Foreman, Karin M. Björkman, Craig A. Carlson, Keri Opalk and David M. Karl

---

Supplementary Data

Photographs of the Velacure12 UV system

Ducting to exhaust fan in hood. This cools the light bulb and vents ozone to hood.

Power supply and control station.

Ice bath for cooling TDP samples during UV irradiation. Pressurized house air, supplied from hood, is regulated to 20 psi, flows through ice bath and enters the bottom port in back of the light chamber.

Sample chamber with UV reflective coating.

UV light assembly with microwave, cooling fan and UV bulb.

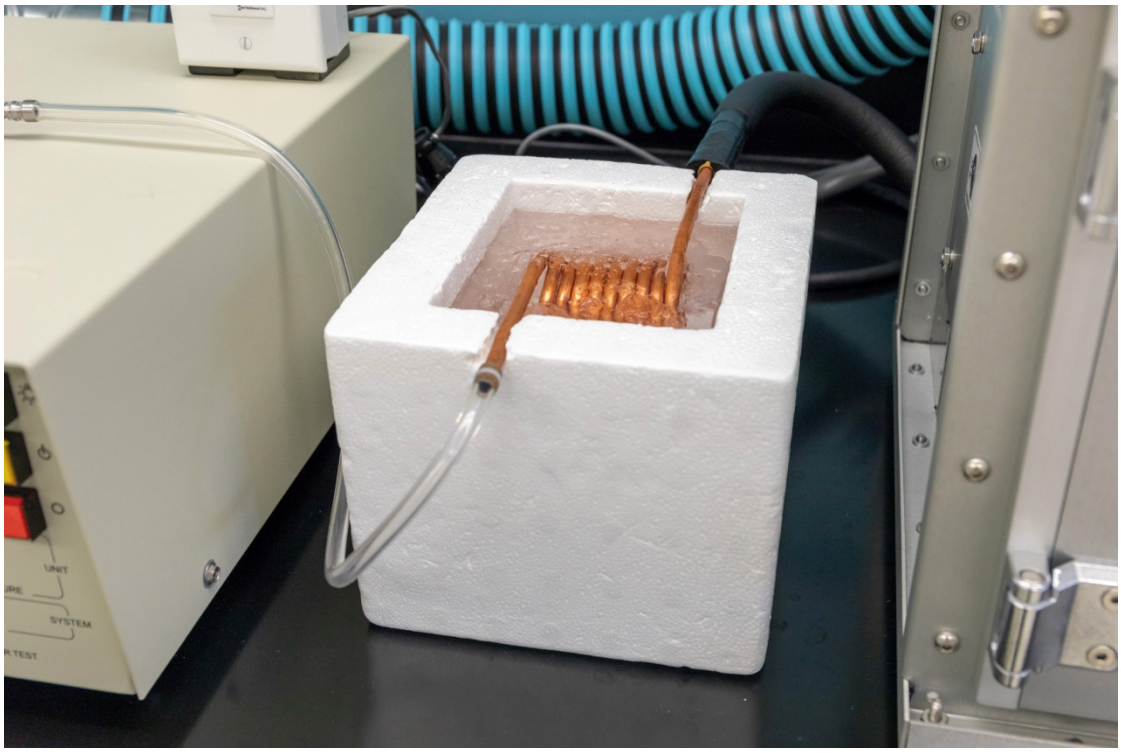

Cooling air line through ice bath, for use with TDP sample runs. Not used for TDN sample runs.

Rear of system, showing sample cooling air going into the bottom back port of the light chamber and 3 in. ducting extending from the light assembly and heading to the exhaust/cooling fan in the hood.

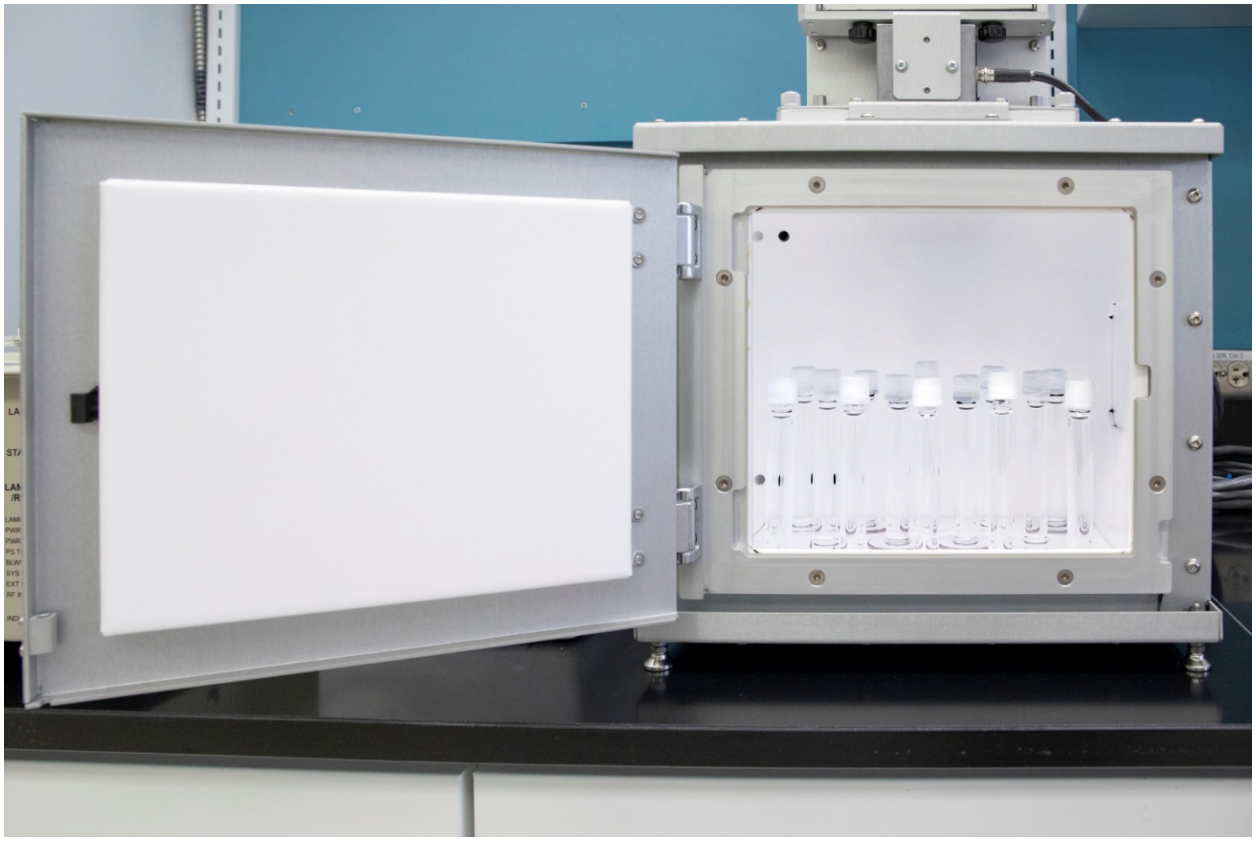

Sample vials in the light chamber (top and bottom left) and with a ruler for scale (right). Caps are wrapped with PTFE tape to increase reflectance and thereby minimize heating of the vials during UV irradiation. A typical TDP run has 18 vials in the light chamber and a typical TDN run has 24 vials.

Depth profiles of particulate C, N and P at Station ALOHA, North Pacific Subtropical Gyre
Samples are from HOT cruises 1 – 298 (spanning ~30 years)
Data available through the HOT-DOGS database:
http://hahana.soest.hawaii.edu/hot/hot-dogs/index.html
Error bars represent 1 standard deviation of the data

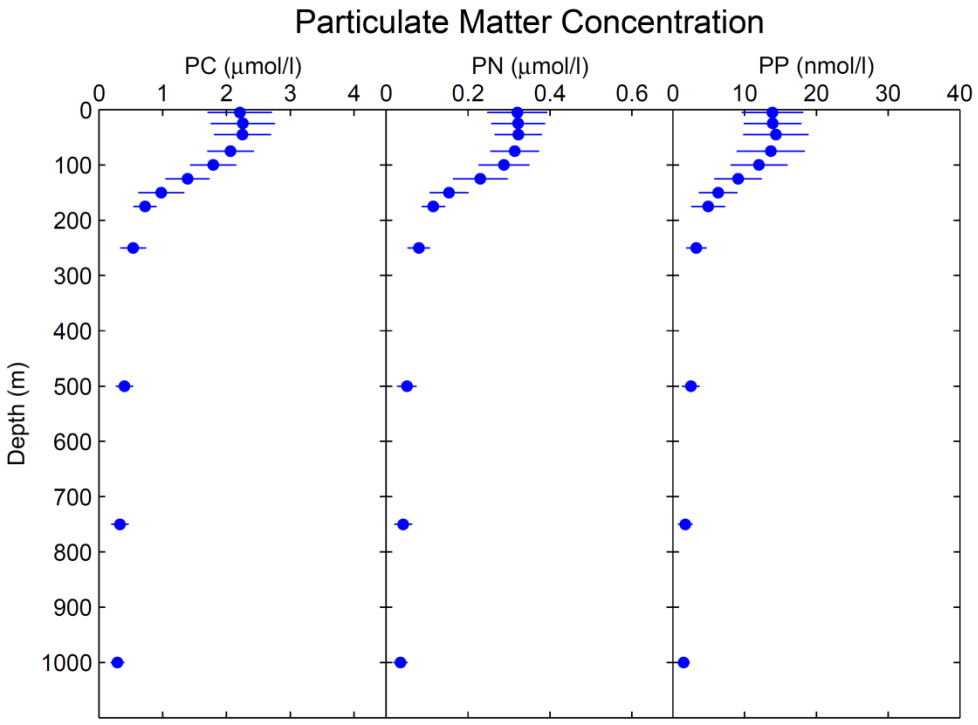

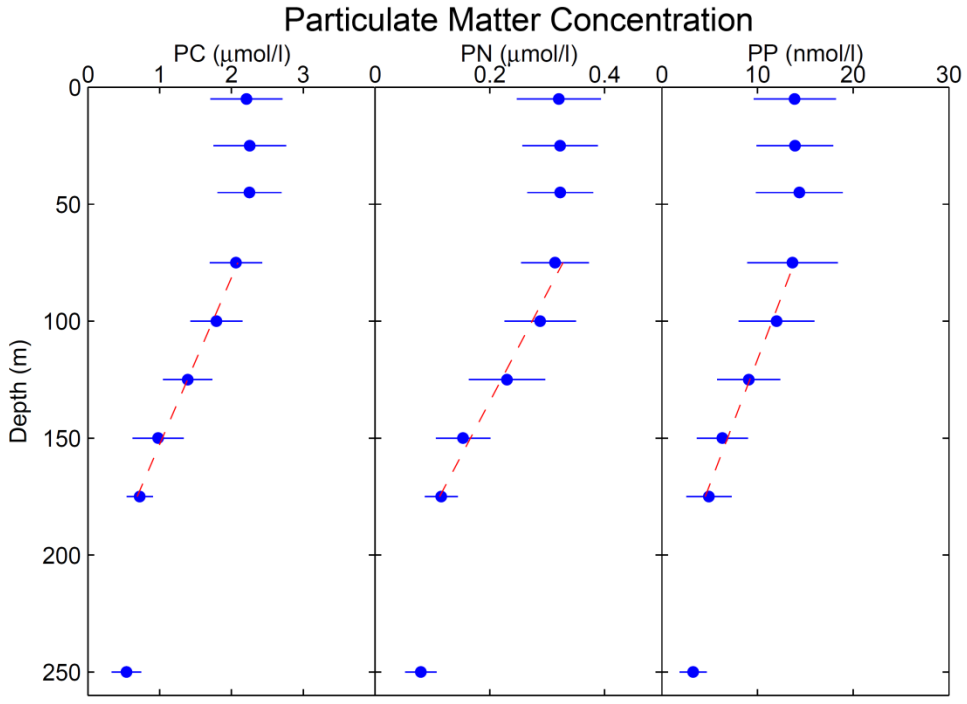

Updated from Hebel and Karl (2001)